25. M. J. Berridge and R. F. Irvine, *Nature (London)* **312**, 315 (1984); Y. Sugimoto and R. L. Erikson, *Mol. Cell. Biol.* **5**, 3194 (1985); S. Jackowski, C. W. Rettenmier, C. J. Sherr, C. O. Rock, *J. Biol. Chem.* **261**, 4978 (1986).
26. P. W. Majerus *et al.*, *Science* **234**, 1519 (1986); R. M. Bell, *Cell* **45**, 631 (1986); Y. Nishizuka, *Science* **233**, 305 (1986).
27. M. R. Smith, S. J. DeGudicibus, D. W. Stacey, *Nature (London)* **320**, 540 (1986).
28. R. Jaggi, B. Salmons, D. Muellener, B. Groner, *EMBO J.* **5**, 2609 (1986).
29. A. Schmidt, C. Setoyama, B. de Crombrugghe, *Nature (London)* **314**, 286 (1985); M. S. Rabin, P. J. Doherty, M. M. Gottesman, *Proc. Natl. Acad. Sci. U.S.A.* **83**, 357 (1986).
30. The *ras*-transformed cell line NZ61.8L was analyzed at passage 4. The serine/threonine kinase gene transformed cells Mos 1, 2 and 3 were passage 6, while v-*raf* and A-*raf* lines were 19th and 9th passage, respectively. Tyrosine kinase gene transformed lines Src 1, Fes 1 and Fms 1 were low, but undefined passage number. Src 2 was tested at passage 3. Nuclear oncogene transformed lines NIH/hmyc 1, NIH/p53.3 were passage 4 and 6, respectively, and VM 1, 4 and 5 were passage 3. NIH 3T3 clone 7 was passaged a total of 16 times. Of the above-listed cells, we isolated and tested lines freshly transformed by ser/thre kinases (Mos 1, 2, and 3), tyr kinases (Src 2), as well as nuclear oncogenes (VM 1, 4, and 5). Data from these cell lines were identical with results from cells provided by other laboratories.
31. We wish to thank G. M. Cooper (NZ61.8 cells), U. R. Rapp (NIH/F4-3611, NIH/91V#5, NIH 3T3 clone 7), J. E. Dick (ψ2), S. M. Anderson (Src 1), J. Even (Fes 1), C. J. Sherr (Fms 1), and M. D. Cole (NIH/hmyc1 and NIH p53.3) for the generous gift of cell lines. We are also very grateful for the use of MX2122-B31/NEO supplied to us by M. Verderame together with M. Scott and H. E. Varmus, as well as G. P. Dotto and R. A. Weinberg, for the use of VM retrovirus and valuable advice. Supported by the National Cancer Institute of Canada, The Manitoba Health Research Council, and The Winnipeg Children's Hospital Research Foundation. S.E.E. is supported by a Steve Fonyo National Cancer Institute of Canada Studentship. A.H.G. and J.A.W. are Terry Fox Cancer Research Scientists.

An Amylose Antiparallel Double Helix at Atomic Resolution

W. HINRICHS, G. BÜTTNER, M. STEIFA, CH. BETZEL,* V. ZABEL,† B. PFANNEMÜLLER, W. SAENGER

In the crystal structure of the polyiodide complex (*p*-nitrophenyl-α-maltohexaose$_2$) · $Ba(I_3)_2$ · $22H_2O$, the maltohexaose units form an antiparallel, left-handed double helix with O-2 ··· O-3 and O-6 ··· O-6 hydrogen bonding and a central cavity that encloses two triiodide units. This structure contrasts with the parallel, left-handed double helix with no central cavity proposed for the A- and B-starch helix and the left-handed single helix in V-amylose and may be relevant for the stabilization of glycogen structure.

STARCH, THE STORAGE POLYSACCHARIDE for glucose in plants, is composed of D-glucopyranose units. It can be separated into the branched amylopectin, which has interglucose bonds of the α(1→4) and α(1→6) type, and the linear amylose, which has exclusively α(1→4) links. Although there is no detailed information on the three-dimensional structure of amylopectin, a series of models have been proposed that suggest that the native crystalline amylose that is deposited in the granules of the cereals (A form) and the tubers (B form) consists of a double helix with intertwined, parallel chains (*1*). On the basis of x-ray fiber diagrams and model building, this double helix was originally proposed to be right-handed (*2*). However, a recent study that combined electron diffraction on microcrystals and single crystal data on methyl-α-maltotrioside (*3*) indicated that it should be left-handed (*4*). In addition, various left-handed single-stranded helices are formed by chemical derivatives of amylose and by complexation of amylose with ionic or molecular guest molecules into the central cavity of the helix (Table 1).

Because these previous structural studies relied mainly on the combination of x-ray fiber diffraction and model building and thus are somewhat controversial (*2–6*), it is necessary to obtain more detailed data from single crystals of oligomers larger than the di- (*7, 8*) and trisaccharides (*3*) that have not been available. In only one case, the complex of maltoheptaose with the enzyme phosphorylase a, was the structure of a larger amylose fragment elucidated (*9*) from single crystal data, albeit at medium resolution (2.5 Å). We report the detailed crystal structure of a longer oligomer of amylose, a maltohexaose that is blocked at the reducing end with a *p*-nitrophenyl group and cocrystallized with barium triiodide. Our study provides information on the structure of a left-handed antiparallel double helix of amylose complexed with polyiodide.

We were unable to crystallize maltooligomers in a form suitable for x-ray analysis [see also (*10*)], and resorted to derivatives in which the reducing end was blocked by a *p*-nitrophenyl group in the α-position. Because α-cyclodextrin polyiodide complexes crystallize in a variety of space groups depending on the cation (*11*), we mixed aqueous solutions of the commercially available (Boehringer Mannheim) maltooligomer derivatives with a series of metal iodides and iodine. Addition of BaI_2 and iodine to *p*-nitrophenyl-α-maltohexaose immediately yielded a fine, brown powder. Brown plates from this material suitable for single crystal

Table 1. A selection of parameters for helical structures formed by amylose and its derivatives (*1, 9*).

Structure of amylose or derivative	Helix					
	Type*	Handedness	Pitch height (Å)	Number of residues per turn	Rise per residue (Å)	Helix diameter‡ (Å)
A	DP	Right†	21.04	6	3.51	10.66
B	DP	Right†	20.80	6	3.47	10.68
V_h	S	Left	8.05	6	1.34	13.70
V_h-iodine	S	Left	8.17	6	1.36	13.54
KOH	S	Left	22.41	6	3.74	7.58
KBr	S	Left	16.52	4	4.13	7.21
Amylose triacetate	S	Left	52.53	14	3.75	10.87
Trimethyl amylose	S	Left	15.64	4	3.91	9.66
Heptaamylose in complex with phosphorylase a	S	Left	15.8	6.6	2.3	
Idealized helix (this work)	DAP	Left	18.6	8.0	2.33	14.8

*Abbreviations: S, single; DP, double, parallel; DAP, double, antiparallel. †In a recent electron diffraction study (*4*), a left-handed double helix was proposed. ‡Taken as the interchain spacings in (*1*) for amylose helices and as van der Waals diameters for the double helix derived from *p*-nitrophenyl-α-maltohexaose (this work).

W. Hinrichs, G. Büttner, M. Steifa, Ch. Betzel, V. Zabel, W. Saenger, Institut für Kristallographie, Freie Universität Berlin, Takustrasse 6, D-1000 Berlin 33, Federal Republic of Germany.
B. Pfannemüller, Institut für Makromolekulare Chemie, Universität Freiburg, Stefan-Meier-Strasse 31, 7800 D-7800 Freiburg, Federal Republic of Germany.

*Present address: European Molecular Biology Laboratory, Hamburg Outstation, c/o DESY, Notkestrasse 85, D-2000 Hamburg 52, Federal Republic of Germany.
†Present address: Oak Ridge National Laboratory, Oak Ridge, TN 37831.

x-ray diffraction studies could be obtained when a solution near precipitation conditions was sealed in a melting point capillary and left for a few days.

The space group of these crystals is orthorhombic, $P2_12_12_1$. The unit cell constants are $a = 33.732(13)$, $b = 29.212(10)$, $c = 14.442(4)$ Å. (Numbers in parentheses are standard deviations in the last decimal digit or digits.) We used a four circle diffractometer (nickel-filtered Cu K_α radiation) to collect about 10,000 x-ray intensity data, which were corrected for absorption (*12*). The heavy-atom positions were derived by Patterson methods; all other nonhydrogen atoms were located from difference Fourier maps. Least-squares refinement (*13*) converged at a conventional *R*-factor of 0.11 with the heavy atoms treated anisotropically and the others isotropically. The crystal asymmetric unit contains two *p*-nitrophenyl-α-maltohexaose and two triiodide units, one barium ion, and 22 water molecules $[(C_{42}H_{65}O_{33}N)_2 \cdot Ba(I_3)_2 \cdot 22H_2O]$.

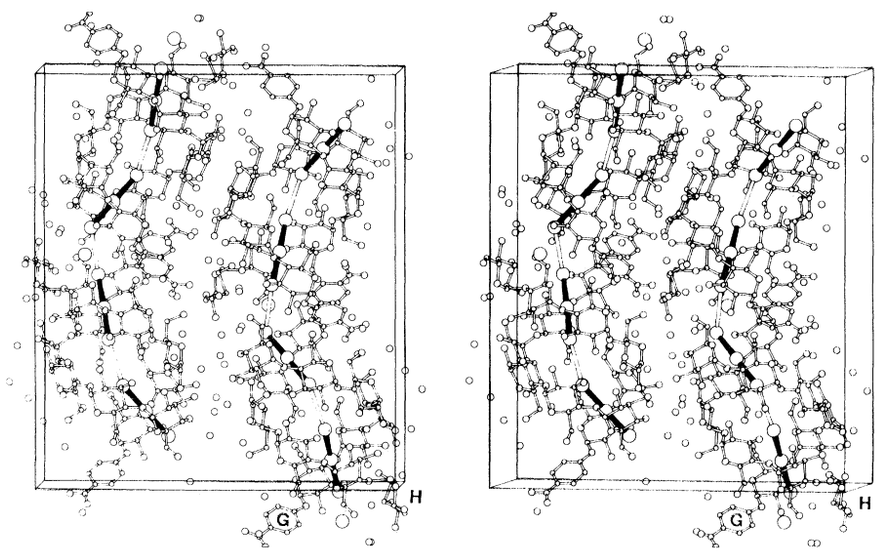

Fig. 1. Stereoview [produced with the ORTEP program (*31*)] along the crystallographic **c**-axis of the unit cell of (*p*-nitrophenyl-α-maltohexaose)$_2 \cdot Ba(I_3)_2 \cdot 22H_2O$; **a**-axis vertical, **b**-axis horizontal. The phenyl ring G of **1** and the glucose H of **2** are indicated. Solid lines are the covalent bonds in the triiodides, whereas the open lines are intertriiodide contacts. Atoms with increasing radius represent carbon, nitrogen, oxygen, iodine, and barium.

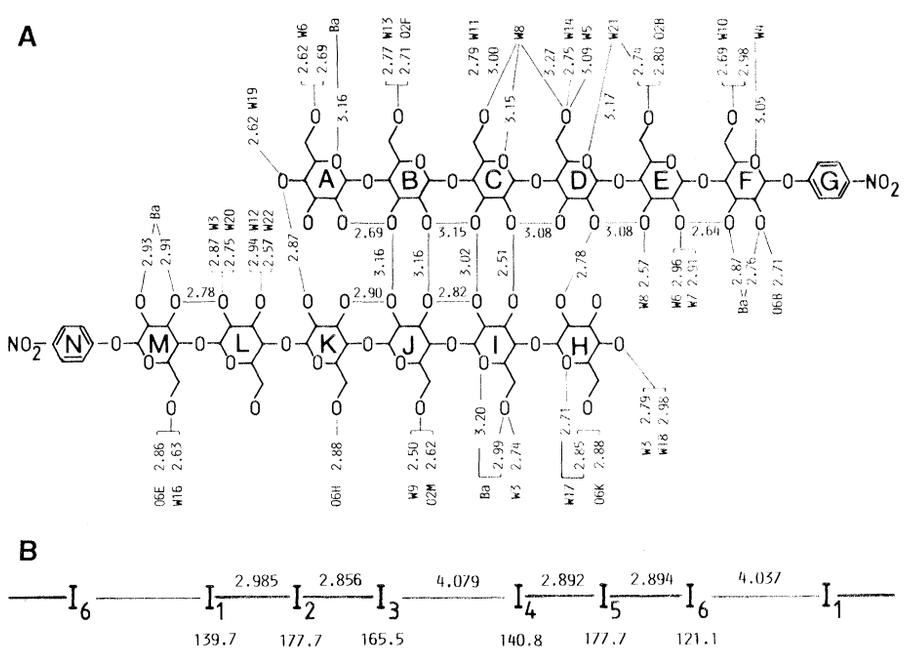

Fig. 2. Schematic illustration of hydrogen-bonding and barium-ion coordination interactions in the double helical complex, including water molecules (**A**) and interatomic bond angles and distances in the polytriiodide chain (**B**). The standard deviations are 0.02 Å in O ··· O distances and 0.007 Å and 0.2° in triiodide distances and angles, respectively. The average distance along the polyiodide chain, 3.29 Å, is significantly longer than the 3.11 Å in blue starch iodine (*17*) and in the (α-cyclodextrin)$_2 \cdot CdI_5$ complex (*11*). Glucoses A to F are in **1** and glucoses H to M are in **2**; W indicates water molecules. There is one direct intermolecular contact between the O-6 hydroxyls of E and M of 2.86 Å.

The dominant motif of this crystal structure is a polytriiodide zigzag chain with $(I_3^-)_2$ as the repeating unit embedded in the central cavity of a left-handed, antiparallel double helix that is formed by two symmetry-independent *p*-nitrophenyl-α-maltohexaose molecules. The twofold screw axis operation parallel to **a** creates a continuous although wavy array of these double helices, which are interlocked with their terminal *p*-nitrophenyl groups (Fig. 1).

In the *p*-nitrophenyl-α-maltohexaose double helix the two enclosed triiodide units have dimensions similar to those in other triiodide crystal structures (*14, 15*). They are separated by 4.08 Å and form an angle of 140.8° (Figs. 2 and 3). The distance between triiodides in adjacent asymmetric units is comparable but the angle is reduced to 121° and follows the bend between the short double helices (Fig. 1).

The angles formed by the triiodide units lie between the approximate right angle observed in polyiodides that are crystallized with inorganic or small organic cations (*14, 15*) or that are complexed with β-cyclodextrin (*16*) as the matrix and the linear polyiodide that occurs when triiodide is embedded in the narrow channels formed by α-cyclodextrin (*11*) or by the V-amylose helix (*17*) in "blue starch iodine." In these latter complexes the distance between the triiodide units is about 1 Å shorter than the van der Waals separation (*18*) of 4.3 Å, which suggests that the deep blue or black color is due to charge transfer (*17, 19*). The brown color of the *p*-nitrophenyl-α-maltohexaose polyiodide crystals indicates that these interactions are unlikely to occur in the zigzag polyiodide arrangement with an intertriiodide separation of ~4 Å, and that this complex is a poor model for blue starch iodine.

In each of the ribbonlike maltohexaose molecules **1** and **2** (Figs. 2 and 3), the O-2, O-3 hydroxyls are on one edge of the ribbon and are so close that intramolecular, interglucose O-2 ··· O-3′ hydrogen bonds either can form or could form if the glucose units were rotated slightly about the glucosidic links. Based on O ··· O distances, all the possible interglucose O-2 ··· O-3′ hydrogen bonds occur in **1**, which forms a more regular helical segment than **2** and in which close O-2 ··· O-3′ contacts are only found between the glucoses I and J, J and K, and L and M. The other edges of the *p*-nitrophenyl-α-maltohexaose ribbons are lined by the O-6 hydroxyls, all of which are oriented

gauche,gauche as is usually observed in cyclodextrins (*20*).

The more regular appearance of **1** is also manifested in the torsion angles Φ and Ψ (Table 2), which describe the relative rotation of the glucose units about the glucosidic C-1–O-4′–C-4′ links. These angles are near the average values of $\Phi' = 160(4)°$, $\Psi' = 170(5)°$ in **1** but are more spread for **2**, especially in those sections where the O-2 ··· O-3′ separation is wider than expected for hydrogen bonding.

In a double helix, each repeat unit in one strand has a partner unit in the other strand. In the *p*-nitrophenyl-α-maltohexaose double helix, glucoses A to D in **1** have partner glucoses H to K in **2**. The other glucoses are out of frame and are in hydrogen-bonding contact with water molecules and coordinated to barium ions (Figs. 2 and 3).

Of the eight juxtaposed glucoses, only the four central units are close enough so that four intermolecular hydrogen bonds O-2 ··· O-3 can form. Between the O-6 hydroxyls there is one direct short intermolecular O-6 ··· O-6 hydrogen-bonding contact of 2.86 Å between glucoses E and M. A second interaction between the O-6 groups of glucoses F and L would be possible if L were slightly rotated.

This hydrogen bonding between O-2, O-3 hydroxyls on one side and between O-6 hydroxyls on the other contributes significantly, if not primarily, to helix stabilization. It occurs systematically in an idealized double helix whose structural parameters (Table 1 and Fig. 4) were derived mathematically (*21, 22*) with the atomic coordinates of the O-4 atoms of the central part of **1**. This double helix is novel because the A- and B-amylose double helices have parallel strands and do not exhibit a central cavity, and because the helices formed by V-amylose and by amylose derivatives are only single stranded (*1–6*).

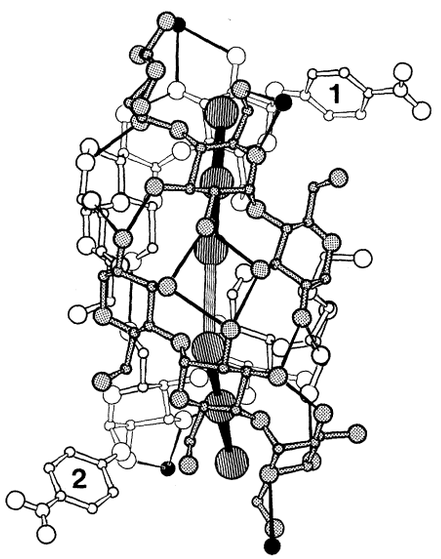

Fig. 3. View of the molecular complex (*p*-nitrophenyl-α-maltohexaose)$_2$ · Ba(I$_3$)$_2$ [plotted with the program SCHAKAL (*32*)]. Hydrogen bonds, interiodine covalent bonds, and the Ba–O coordinative bonds are drawn black. Molecules **1** and **2** are indicated by numbers in the *p*-nitrophenyl groups. Parts of the molecular complex closer to the viewer are stippled. The triiodide contact bond is drawn shaded. Carbon, barium, nitrogen, oxygen, and iodine atoms are indicated by increasing radii; barium ions are filled black. Water molecules are omitted for the sake of clarity.

However, the parameters derived for the idealized antiparallel left-handed amylose double helix are comparable to parameters obtained for the left-handed amylose single helix (*9*) of maltoheptaose complexed with the enzyme phosphorylase a. This helix is somewhat slimmer and has 6.6 residues per turn with a pitch of 15.8 Å. It was used as a basis for modeling a double helix with 6 glucoses per 18 Å pitch and with glucosidic torsion angles of $\Phi' = -15°$ and $\Psi' = -26°$. Compared with our idealized double helix, the number of glucoses per turn is different, and the values of the Φ′ and Ψ′ angles are reversed (see Table 2).

The crystal structure is stabilized by several interactions. First, **1** and **2** are held together by hydrogen bonds. Second, the terminal *p*-nitrophenyl moieties of adjacent units interlock and stack at a phenyl-to-phenyl distance of 3.2 Å, which leads to the "infinite-chain" arrangement shown in Fig. 1. Third, the triiodide units interact to form an infinite polyiodide. Fourth, each barium ion coordinates to two water molecules and to four chelating glucoses (A, F, I, and M) of four different maltohexaose molecules. Finally, the 22 water molecules are mainly in hydrogen-bonding contact with the terminal glucoses A, E, and F and H, L, and M.

Maltohexaose is the linear analog of the cyclically closed cyclodextrins that were studied by x-ray and neutron diffraction (*20*). Comparison of average geometrical data in Table 2 suggests that cyclization opens the C-4–O-4′–C-1′ angle from 115(3)° in maltohexaose to 119.0(7)° in α-cyclodextrin. The average O-4 ··· O-4′ virtual bond distance of the glucose unit decreases from 4.52(9) Å in maltohexaose to 4.23(6) Å in α-cyclodextrin. However, the intramolecular, interglucose O-2 ··· O-3′ hydrogen-bonding distance is larger in α-cyclodextrin, 3.00(8) Å, than in the maltohexaose molecule, 2.89(20) Å.

These data indicate that the glucose geometry is mechanically strained in α-cyclodextrin. The virtual bond angles O-4–O-4′–O-4″ average 120(2)° in α-cyclodextrin compared with the average of 138(5)° in the linear analog. The virtual torsion angles O-4–O-4′–O-4″–O-4‴, which are 0° in the cyclodextrins because of ring-closure constraints, range from −5.1° to −128.7° in linear maltohexaose, with the central units in the double-helical arrangement confined in the range from −20.0° to −29.3°. The steric strain diminishes in the series α- > β- > γ-cyclodextrin, and the data in Table 2 for γ-cyclodextrin agree with those for maltohex-

Table 2. Comparison of average structural parameters for amylose fragments in *p*-nitrophenyl-α-maltohexaose and in the cyclically closed analogs α-, β-, and γ-cyclodextrin. Standard deviations in parentheses refer to last decimal digit.

Parameter	*p*-Nitrophenyl-α-maltohexaose*	Cyclodextrin†		
		α	β	γ
Number of glucoses	6	6	7	8
Intramolecular distances (Å)‡				
O-4 ··· O-4′	4.52 (9)	4.23 (6)	4.36 (11)	4.48 (5)
O-2 ··· O-3′	2.89 (20)	3.00 (8)	2.86 (6)	2.81 (7)
Angles (degrees)				
C-1–O-4′–C-4′	115 (3)	119.0 (7)	117.7 (9)	112.6§
O-4 ··· O-4′ ··· O-4″	138 (5)	120 (2)	128 (3)	135 (2)
Torsion angles (degrees)‡‖				
φ′ O-4 ··· C-1–O-4′–C-4′	160 (4)	166 (5)	169 (5)	167 (4)
ψ′ C-1′–O-4′–C-4′ ··· O-4″	170 (5)	−169 (11)	−171 (8)	−170 (4)
φ H-1–C-1–O-4′–C-4′	−19 (6)			
ψ C-1–O-4′–C-4′–H-4′	−12 (7)			
O-4 ··· O-4′ ··· O-4‴ ··· O-4‴		0	0	0
1	−5.1; −21.8; −29.3; −40.3			
2	−128.7; −24.6; −20.0; −75.7			

*Averaged data for **1** and **2** except for last entries; these entries have SD = 0.01°. †Data from (*27–29*). ‡Values from computer-built models for O-4 ··· O-4′; O-2 ··· O-3′; φ, ψ values are for the following amylose polymorphs: V$_6$, 4.25 Å, 2.75 Å, −14°, −6°; V$_7$, 4.21 Å, 2.78 Å, −18°, −3°; KBr, 4.57 Å, 4.51 Å; −60°; −41°; KOH, 4.57 Å, 2.93 Å, −3°, −33°. Native A and B amylose double helix: 4.48 Å, 3.35 Å, −28°, −5° [data from (*30*)]. §No standard deviations are given because the data are based on incomplete refinement. ‖φ′, ψ′ and φ, ψ refer to two different definitions used in the literature. The given average values are only for those glucosidic links where O-2 ··· O-3′ hydrogen bonds are formed, that is, values for glucose pairs H, I and K, L are omitted from averaging.

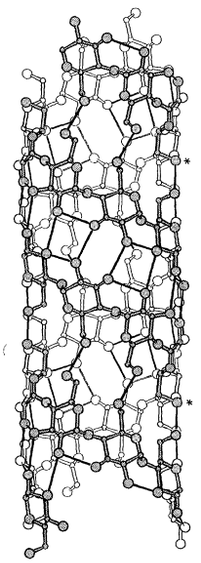

Fig. 4. Drawing of the idealized amylose antiparallel double helix derived on the basis of glucose residues C and D in **1** (*32*). Helix parameters are given in Table 1; the pitch height is indicated by the asterisks. Van der Waals diameters for the central cavity and for the outer-helix boundaries are 4.9 Å (C-6–H atoms) and 15.9 Å (O-2 and O-3 atoms), respectively, and are comparable to dimensions known for α-cyclodextrin (*11*). The O-2 ··· O-3 and O-6 ··· O-6 hydrogen bonds are indicated in black; the atomic code is as in Fig. 3.

aose if we neglect the virtual torsion angles.

The solution properties of cyclic and linear oligosaccharides differ dramatically. Whereas the α-, β-, and γ-cyclodextrins display limited solubility in water, with β-cyclodextrin being the least soluble (1.85 g in 100-ml solution) (*20*), the linear analogs are virtually indefinitely soluble. Evaporation of aqueous solutions of linear oligosaccharides yields glasses, whereas cyclodextrins crystallize.

The antiparallel double helix found in this crystal structure is probably limited to maltooligomers of finite length because two chains of opposite polarity must intertwine. This topological problem is comparable to that for DNA. However, in DNA the geometry of the base pairs imposes antiparallel polynucleotide strands (*23*), and the double helix is stabilized by hydrophobic and dispersion forces between the base pairs, which are stacked in the core of the helix. In the amylose double helix, the polyiodide chain can initially stabilize a structure by forming a nucleus around which the amylose chains can wind; in addition, intermolecular hydrogen bonds of the type O-2 ··· O-3 and O-6 ··· O-6 can increase the stability of the complex. Such intermolecular hydrogen bonding was observed in crystal structures of α-, β-, and γ-cyclodextrins (*20*) and appears to be the most preferred amylose-amylose interaction.

With amylose chains of infinite length, the antiparallel double helix is not favored because chains must intertwine and single helices become more probable. The interactions that stabilize the single helices are hydrophobic forces between amylose and guest molecules, intrachain hydrogen bonds between adjacent glucoses O-2 ··· O-3′, and interturn hydrogen bonds O-2 ··· O-6 and O-3 ··· O-6. These latter hydrogen bonds are only rarely seen in cyclodextrin crystal structures (*20*), probably because intermolecular O-2 ··· O-3 and O-6 ··· O-6 interactions are more favorable; in amylose, this energetic disadvantage could be compensated by the topological advantages of single helix formation.

The amylose antiparallel double helix may be significant when only short helical segments are formed so that topological problems are largely avoided. Because of the similarity of conformational and helical parameters in the (maltoheptaose) left-handed single helix (*9*) and in the (maltohexaose) left-handed double helix, the transformation from one helix form to the other can occur readily.

This may be important in glycogen granules that are formed by cascade-like, branched structures with α(1→4) and α(1→6) glucosidic linkages to yield a core macrodextrin (*24*). At the periphery of the macrodextrin there are short segments of amylose that form left-handed single helices with about 6.6 glucoses per turn (*9*). These could easily intertwine to form left-handed antiparallel double helices, and further stabilize the structure of the granules. The short length of these helical segments would easily explain the brown (and not blue) color of complexes between glycogen and iodine. The observed B-type x-ray diffraction of glycogen (*25*) appears to contradict the concept of antiparallel double helix formation. However, the pattern was not obtained from native glycogen; the glycogen required considerable treatment and the pattern could not be reproduced.

Gelation of amylose and starch upon cooling of aqueous solution could be associated with initial formation of short segments of antiparallel double helices between amylose chains. This would result in three-dimensional, loose networks with intertwined amylose chains, which precipitate and are difficult to redissolve.

In the crystal structure of methyl-α-maltotrioside (*3*), the oligomer occurs as a left-handed single helix with axial rise per residue of 3.5 Å, which does not allow intramolecular hydrogen bonding O-2 ··· O-3′ between adjacent glucose units. This structure can be taken as a prototype for amylose helices devoid of intrachain hydrogen bonding, as they exist probably in A- and B-type polymorphs. The parameters of the present antiparallel double helix of *p*-nitrophenyl-α-maltohexaose complexed with polyiodide suggest another helix prototype in which O-2 ··· O-3′ intrachain hydrogen bonding occurs, as observed in all the V-amyloses. Thus far no amylose double helix with parameters comparable to those derived in the present study has been observed (*26*), which suggests that amylose double helices do not form readily. However, in conformational energy calculations, the double helices correspond to an energy minimum (*3*). Thus the structural parameters for two prototype amylose helices are now available at atomic resolution for use in model-building studies to improve the interpretation of the fiber diffraction data.

REFERENCES AND NOTES

1. A. Sarko and P. Zugenmaier, *ACS Symp. Ser.* **141**, 459 (1980).
2. H. C. Wu and A. Sarko, *Carbohydr. Res.* **61**, 7 (1978); *ibid.* **27**.
3. W. Pangborn, D. Langs, S. Pérez, *Int. J. Biol. Macromol.* **7**, 363 (1985).
4. A. Imberty *et al.*, *Macromolecules*, in press.
5. D. A. Brant, *Rev. Biophys.* **9**, 527 (1976).
6. R. Cleven *et al.*, *Starch Staerke* **30**, 223 (1978).
7. F. Takusagawa and R. A. Jacobson, *Acta Crystallogr.* **B34**, 213 (1978).
8. I. Tanaka *et al.*, *ibid.* **B32**, 155 (1976).
9. E. Goldsmith *et al.*, *J. Mol. Biol.* **156**, 411 (1982).
10. D. French, *Jpn. Soc. Starch Sci. J./Denpun Kagaku* **19**, 8 (1972).
11. M. Noltemeyer and W. Saenger, *J. Am. Chem. Soc.* **102**, 2710 (1980).
12. A. C. T. North, D. C. Phillips, F.S. Matthews, *Acta Crystallogr.* **A24**, 351 (1968).
13. G. M. Sheldrick, SHELX76, Department of Chemistry, University of Cambridge, Cambridge, 1976.
14. E. H. Wiebenga, E. E. Havinga, K. H. Boswijk, *Adv. Inorg. Radiochem.* **3**, 133 (1961).
15. K.-F. Tebbe, *Polyhalogen Cations and Polyhalide Anions in Homoatomic Rings, Chains and Macromolecules of Main-Group Elements*, A. L. Rheingold, Ed. (Elsevier, Amsterdam, 1977), pp. 551–606.
16. Ch. Betzel, M. Noltemeyer, G. Weber, W. Saenger, J. A. Hamilton, *J. Inclusion Phenom.* **1**, 181 (1983).
17. T. L. Bluhm and P. Zugenmaier, *Carbohydr. Res.* **89**, 1 (1981).
18. R. C. Weast, Ed., *Handbook of Chemistry and Physics* (CRC Press, Cleveland, 1976), p. D-178.
19. W. Saenger, *Naturwissenschaften* **71**, 31 (1984).
20. ——, in *Inclusion Compounds*, J. D. Atwood, J. E. D. Davies, D. D. McNicol, Eds. (Academic Press, London, 1984), vol. 2, pp. 231–259.
21. T. Shimanouchi and S.-I. Mizushima, *J. Chem. Phys.* **23**, 707 (1955).
22. H. Sugeta and T. Miyazawa, *Biopolymers* **5**, 673 (1967).
23. J. D. Watson and F. H. C. Crick, *Nature (London)* **171**, 737 (1953).
24. W. Burchard, *Adv. Polym. Sci.* **48**, 1 (1983).
25. D. French and S. Kikumoto, *Arch. Biochem. Biophys.* **156**, 794 (1973).
26. ——, in *Starch Chemistry and Technology*, R. L. Whistler, J. N. BeMiller, E. F. Paschall, Eds. (Academic Press, New York, ed. 2, 1984), p. 205.
27. B. Hingerty and W. Saenger, *J. Am. Chem. Soc.* **98**, 3357 (1976).
28. K. Lindner and W. Saenger, *Carbohydr. Res.* **99**, 103 (1982).
29. ——, *Biophys. Biochem. Res. Commun.* **92**, 933 (1980); K. Lindner, thesis, Universität Göttingen, 1980.
30. A. D. French and V. G. Murphy, *Polymer* **18**, 489 (1977).
31. C. K. Johnson, *Rep. ORNL-3794* (Oak Ridge National Laboratory, Oak Ridge, TN, 1965).
32. E. Keller, *Chem. Unserer Zeit* **14**, 56 (1980).

33. B.P., G.B., and W.S. are grateful for financial support by the Deutsche Forschungsgemeinschaft (Az. Sa 196/12-1) and by Fonds der Chemischen Industrie. W.H. and Ch.B. hold fellowships through Sonderforschungsbereich 312 (Teilprojekt D1), and through Bundesministerium für Forschung und Technologie, FKZ: 05 313 IA B. We acknowledge the technical assistance of P. Armbruster and the help in initial data collection by W. Dreißig.

27 February 1987; accepted 7 July 1987